Residual stress effects on piezoelectric response of sol-gel derived lead zirconate titanate thin films

T. A. Berfield
Theoretical and Applied Mechanics Program, Department of Mechanical Science and Engineering, University of Illinois at Urbana-Champaign, Urbana, Illinois 61801

R. J. Ong and D. A. Payne
Department of Materials Science and Engineering, University of Illinois at Urbana-Champaign, Urbana, Illinois 61801 and Frederick Seitz Materials Research Laboratory, University of Illinois at Urbana-Champaign, Urbana, Illinois 61801

N. R. Sottos[a)]
Department of Materials Science and Engineering, University of Illinois at Urbana-Champaign, Urbana, Illinois 61801 and Beckman Institute for Advanced Science and Technology, University of Illinois at Urbana-Champaign, Urbana, Illinois 61801

(Received 18 September 2006; accepted 29 October 2006; published online 16 January 2007)

Piezoelectric properties of three sol-gel derived $Pb(Zr_{0.53}Ti_{0.47})O_3$ thin film specimens of different thicknesses integrated onto $Pt/Ti/SiO_2\|Si$ substrates are investigated to delineate the influence of residual stress on the strain-field response characteristics from other thickness related effects. Residual tensile stresses are determined from wafer curvature measurements for films ranging in thickness from 190 to 500 nm. Field-induced strains are measured interferometrically for each film under either a large ac driving voltage or a small ac ripple applied over a range of dc biases. Higher residual stresses decrease measured piezoelectric response, while thickness variations with no accompanying change in residual stress state produce little change in strain-field behavior. The diminished performance associated with high residual stresses is attributed to reductions in both linear and nonlinear contributions, including decreased polarization switching and domain motion.
 [DOI: 10.1063/1.2422778]

I. INTRODUCTION

The development of enhanced properties in ceramic ferroelectric thin films poses a challenge for future advancements in the areas of integrated, multifunctional microelectronics and micromechanical devices. Although ferroelectric thin films hold tremendous potential for widespread use in miniaturized electronic applications, many previous reports have indicated that the dielectric, ferroelectric, and piezoelectric properties of electroceramic thin films are often vastly diminished compared to their bulk counterparts. As film thickness is pushed towards its lower limits, a factor that gains influence over the ferroelectric properties is the level of processing related residual stress. This study focuses on the potential effects of residual film stress and finite film thickness on the piezoelectric response for polycrystalline $Pb(Zr_{0.53}Ti_{0.47})O_3$ (PZT) thin films.

Residual stresses in electroceramic thin films can be very high but are often neglected due to a lack of adequate stress measuring capabilities. The magnitude and sign (tensile or compressive) of the film stress are highly dependent on both the processing technique and the properties of the substrate and bottom electrode.[1] Tuttle *et al.*[2] and others[3,4] speculate on the influence of residual stress on preferred domain orientation. Assuming that domains align in the most energetically favorable arrangements, populations of non-180° domains are affected by the stress state upon cooling through the Curie temperature. Tuttle *et al.*[5] have asserted that a tensile stress at this point causes more *a*, or 90°, domains to form in order to relieve some of the residual stress. This orientation leads to a reduction in the ferroelectric properties of thin film samples, provided that non-180° motions are minimized. Additionally, the clamping effect caused by residual stresses alters dielectric and piezoelectric behaviors. Lappalainen *et al.*[6] show that increases in residual stress are linked to reductions in dielectric properties and increases in coercive field. Changes in switching behavior have also been observed to accompany residual stress changes induced by either film annealing[1] or applying an external mechanical stress.[7] Lian and Sottos have measured changes in both the field-induced strains and dielectric constants with film thickness, and then used beam bending tests to show that mechanically applied tensile stresses further diminish the ferroelectric response.[8] These results suggest that control of residual stresses during film fabrication may lead to improved electrical and electromechanical properties.

The residual stress state found in films processed via sol-gel deposition has components that are both intrinsic and extrinsic in nature. Intrinsic stresses originate from the constrained densification and shrinkage of the ceramic during the drying and firing stages of processing. The magnitude of shrinkage stresses created is dependent on the relative rates of evaporation, viscous deformation of the solid, and flow of the liquid in the polymeric gel network during the drying

[a)]Author to whom correspondence should be addressed; electronic mail: n-sottos@uiuc.edu

phase.[9] Other intrinsic sources for the PZT system include the formation of intergranular stresses as anisotropic grains grow, as well as the stress caused by the transformation from a cubic to rhombohedral or tetragonal atomic structure that occurs at the Curie temperature. The two main contributors to the extrinsic component of the residual stress are mismatches between the film and substrate thermoelastic coefficients and crystal lattice parameters. The effect of substrate/film property mismatches on residual stress has been well characterized, and changes in substrates for otherwise similar films have correspondingly altered ferroelectric properties.[2] For the PZT film and platinized silicon substrate studied in this work, the extrinsic forces result in a residual tensile film stress upon cooling.

In addition to mechanical stress effects, the observed changes in both dielectric and piezoelectric properties that accompany the decrease in size scale for PZT thin films have been attributed to a "thickness effect."[10–13] This phenomenon encompasses a combination of factors that are related to film thickness and processing technique. Chief among these variables are grain size, phase type, domain orientation, surface texture, and interfacial effects. Each of these factors has been documented to have a significant effect on final ferroelectric film properties.[14–16] In the current research, we investigate the influence of residual stress on sol-gel derived $Pb(Zr_{0.53}Ti_{0.47})O_3$ thin films of varying thicknesses integrated onto $Pt/Ti/SiO_2\|Si$ substrates. Experimental conditions are carefully controlled to produce films of constant chemical composition, phase content, grain size, and crystallographic orientation to probe the isolated effects of stress and thickness on field-induced strains. Wafer curvature measurements, combined with cross-sectional scanning electron microscopy, enable the determination of residual stresses in the thin films. The stress state in the films is correlated with interferometrically measured strain loops under two different driving conditions of the applied field.

II. EXPERIMENTAL PROCEDURE

Three $Pb(Zr_{0.53}Ti_{0.47})O_3$ thin film specimens ranging in thickness from 190 to 500 nm were prepared by a polymeric sol-gel route. Final film thicknesses were achieved through a buildup of spin cast PZT sol-gel layers. Specifically, samples consisting of 4, 8, and 12 layers were investigated, resulting in crystallized films of 190, 350, and 500 nm thicknesses.

A. Film deposition

The solution chemistry that was employed follows the synthesis route developed by Budd *et al.*[17] and later refined by Lakeman and Payne,[18] for the fabrication of Pb-based perovskite thin films on a substrate. The substrate consisted of a single-side polished Si (100) wafer with a 5000 Å thermally grown oxide and a nominal thickness of 375 μm (Silicon Quest International, Inc., Santa Clara, CA). For the bottom electrode, Ti (300 Å) and Pt (1700 Å) were dc sputtered (in Ar) onto the silicon wafer using an AJA International cosputtering system.

PZT thin films were deposited by spin casting (Headway Research Inc., Garland, TX) onto the platinized silicon substrates from partially hydrolyzed sols dispensed through a filtered syringe. Solution was metered onto a rotating substrate at 300 rpm before accelerating to 3000 rpm for 60 s, producing a layer of uniform coverage. After spin coating, hot-plate treatments in air at 120 °C for 1 min and 300 °C for 1 min, were used to dry and pyrolyze the deposited layer. The spin/hot-plate process was repeated four times, with a subsequent PbO cover coat before firing in a preheated box furnace at 650 °C for 30 min. This sequence of spin casting and heat treatment in four layer increments was repeated to build up the thicker 8 layer (350 nm) and 12 layer (500 nm) films. Full details of the film solution chemistry and casting procedure have been previously published.[19]

B. Residual stress measurement

The average in-plane residual stress in the films was determined by *ex situ* wafer curvature measurements using a KLA-Tencor FLX-2908 laser reflectance system. The Stoney equation was used to calculate the residual stress (σ) in the film from the change in wafer curvature (R) with respect to a carefully measured base line value (R_0),

$$\sigma = \left(\frac{E_s}{1-\nu_s}\right)\frac{t_s^2}{6t_f}\left(\frac{1}{R}-\frac{1}{R_0}\right). \quad (1)$$

This well known equation is valid only in the thin film regime ($t_s \gg t_f$). Hence, the calculation of residual stress in the film only requires knowledge of substrate Young's modulus (E_s) and Poisson's ratio (ν_s) and does not rely on the material properties of the film.

An initial curvature measurement was taken after metallization of the substrate but prior to film deposition. This measurement of the base line curvature for the as-deposited $Pt/Ti/SiO_2\|Si$ substrate does not account for the stress change due to Pt–Ti interactions in the bottom electrode during the heat treatment process. Spierings *et al.*[1,20] and Zhang *et al.*[21] have reported on the need for correction of the base line curvature (R_0) when determining residual stresses in PZT films deposited on $Pt/Ti/SiO_2\|Si$ substrates. Following a process described in detail by Ong *et al.*,[22] at least two identical $PZT/Pt/Ti/SiO_2\|Si$ specimens were fabricated (at each thickness) so that one could be used for further analysis, and the other could have the PZT film removed by an etchant, to reveal the radius of curvature of the heat-treated $Pt/Ti/SiO_2\|Si$ substrate alone. Removal of the PZT thin film was achieved with a solution of hydrochloric acid and ammonium bifluoride in water. The etching process resulted in the recovery of a clean $Pt/Ti/SiO_2\|Si$ substrate with a mirrorlike finish suitable for characterization via laser reflectance. In this manner, the true residual stress in the PZT thin films was calculated via the Stoney method from the change in measured radii of curvature combined with film/substrate thickness measurements obtained from scanning electron microscopy (SEM) micrographs (Fig. 1).

C. Microstructural and phase analysis

Microstructure and phase development were analyzed at room temperature for heat-treated thin films by x-ray diffraction (XRD, Philips X'Pert MRD, Cu $K\alpha$ radiation) and scan-

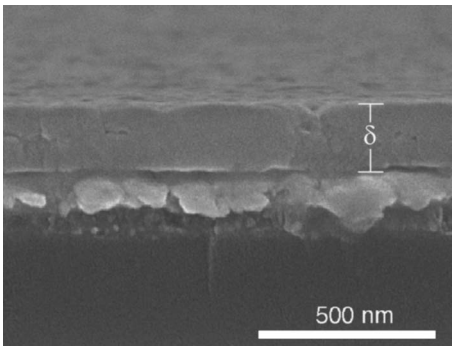

FIG. 1. A SEM micrograph of the film cross section is used to measure the thickness δ of the 190 nm specimen (from Ref. 19).

ning electron microscopy (Hitachi S-4700), which also enable accurate thickness measurements for the heat-treated PZT thin films. SEM micrographs indicated that all three specimens tested were nearly identical in terms of grain size, texture, and microstructure. From plan-view SEM micrographs (Fig. 2), the grain boundaries were identified and an image analysis program (ImageJ, National Instruments) was used to calculate the average grain area for over 160 individual grains on each film. For comparison between films, an assumption of circular grains resulted in calculated average grain diameters of 124, 125, and 122 nm for the films with thicknesses of 190, 350, and 500 nm, respectively. Furthermore, x-ray diffraction testing, presented in full for the same films by Ong *et al.*,[22] confirmed that phase-pure perovskite existed for all three films.

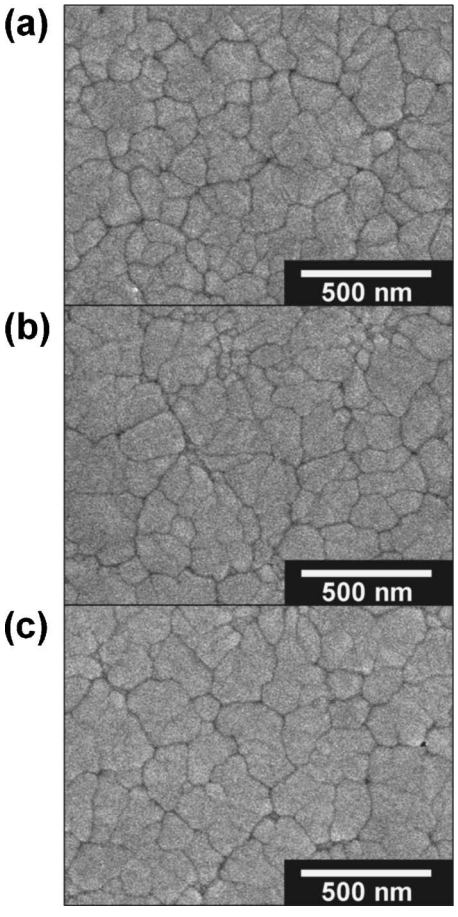

FIG. 2. Plan-view SEM micrographs of the 190 nm (a), 350 nm (b), and 500 nm (c) films. Note the consistency in grain size between films.

D. Interferometric measurements

A portion of each PZT film was chemically etched off in order to expose the bottom electrode. A shadow mask was used to sputter deposit reflective Pt top electrodes that were 1.2 mm in diameter and 2000 Å in thickness. Specimens were then mounted on 1/2 in. thick copper blocks with a rigid bonding agent, and the electrodes were connected with fine copper wire and silver epoxy.

A single-beam heterodyne interferometer system developed by Lian and Sottos[23] measured out-of-plane velocities at the specimen electrode surface. In the sample arm of the interferometer, the beam was sharply focused on the center of the electrode being driven. This reflected beam was then combined with a 40 MHz frequency shifted reference beam at an incident, stationary photodetector. Surface velocities at the electrode face were discerned from the corresponding Doppler frequency shifts in the intensity of the converging beams. These shifts were decoded from the signal output of the photodetector by a FM demodulator in a vibrometer controller (Polytec OFV 3001). The surface velocities were then integrated to find displacement amplitudes.

Piezoelectric strain-field loops were recorded for each of the specimens under two different driving conditions. For the first set of experiments, a large ac electric field was applied at a frequency of 1.0 kHz. The applied voltages to drive the films at 15.0, 20.0, and 30.0 MV/m were based on SEM thickness measurements. A Lecroy LC584A oscilloscope performed a 5000 point, 10 000 sweep time average to record the corresponding velocity and applied voltage data. For the second set of experiments, a large dc bias with a small overlapping ac ripple (1.0 MV/m) was applied across the films. A lock-in amplifier (Stanford Research Systems, model SR 830) demodulated onto the velocity signal amplitude. For each level of applied dc bias, the oscilloscope was once again used to average the velocity amplitude over 1000 sweeps. Prior to the PZT film measurements, a single-crystal quartz sample was tested to determine the accuracy and the displacement resolution for the interferometer. The measured piezoelectric coefficient for the quartz sample was compared with the standard d_{33} value of 2.3 pm/V for a range of driving voltages.[24] As the magnitude of the applied voltage decreased, the experimental d_{33} values consistently matched the standard value until the displacement dropped below 10 pm. At this point, the velocity signal output was comparable to the background noise of the system.

III. RESULTS

Wafer curvature measurements, which were reproducible to within 0.15% for each film, were used to calculate the residual stress for the 190, 350, and 500 nm specimens. The results, summarized in Table I, include bounds based on a worst-case error assumption for each term used in the calculation of stress via (1). All films were in a residual state of biaxial tensile stress. The 190 nm specimen had the highest

TABLE I. Residual stress and measured property data for each thickness.

Specimen	Thickness (nm)	Average residual σ (MPa)	ac driven avg. d_{33}[a] (pm/V)	dc bias peak d_{33} (pm/V)	Dielectric constant K'	tan δ
4 layer	190	180 ±6	33	29	800	0.03
8 layer	350	152±5	61	44	1100	0.02
12 layer	500	153±3	65	44	1200	0.02

[a]Average d_{33} values listed were calculated from the slope of displacement loops plotted against the applied ac voltage, while peak d_{33} values were calculated from displacements induced by a small (1.0 MV/m) applied ac ripple over a range of dc bias fields.

residual stress level of the three (180 MPa), while stress in the 350 and the 500 nm specimens was nearly identical (~152 MPa). Thinner films develop higher residual stress due to the dominant effect of the substrate with very different material properties. X-ray diffraction tests revealed a nominal (111) texture for all films. Measurements from SEM micrographs indicated a consistent grain density across each of the thicknesses, with an average grain diameter of ~110 nm based on a linear intercept method.[22] Results from standard dielectric tests performed[25,26] on each specimen using a Precision *LCR* meter (Hewlett-Packard 4824A) are also included in Table I. These values reflect the average of tests taken from a number of electrodes across the specimen. As the film thickness increased, the dielectric constant also increased, while the loss, tan δ, remained nearly constant.[25]

Field-induced displacements for the 350 nm sample driven at increasing ac fields are given in Fig. 3. These piezoelectric loops are consistent with the typical butterfly pattern associated with ferroelectric switching. Average d_{33} values were calculated from the slope of the linear portion of the displacement-voltage curve as indicated in the boxed region of Fig. 3. Evidence of saturation was observed at the highest applied-field strengths. The 190 and 500 nm specimens (not shown) displayed displacement-field behavior similar to that in Fig. 3. Displacement responses of the three sample thicknesses are compared in Fig. 4(a) for the same applied ac field (20.0 MV/m). Consistent with previous studies,[23] the overall displacement decreases with film thickness. The corresponding field-induced strains are shown in Fig. 4(b). The strains produced from the 350 and 500 nm samples were nearly identical, while the 190 nm response was significantly lower.

Results for the case where films were driven by a small ac ripple applied over a range of dc biases are summarized in Fig. 5. For this driving condition, the d_{33} coefficient was calculated directly from the displacement and the applied ac voltage (1.0 MV/m). The d_{33} responses follow the same trend as found for the high ac voltage strain-field loops. The calculated piezoelectric coefficients for the 350 and 500 nm samples were similar, whereas the 190 nm was significantly lower (Table I). Although the same trend exists for both loading situations, the d_{33} values calculated from the slope of the ac driven displacement-field curves were notably higher than those extracted from the dc bias involved method.

A noticeable difference in response between positively

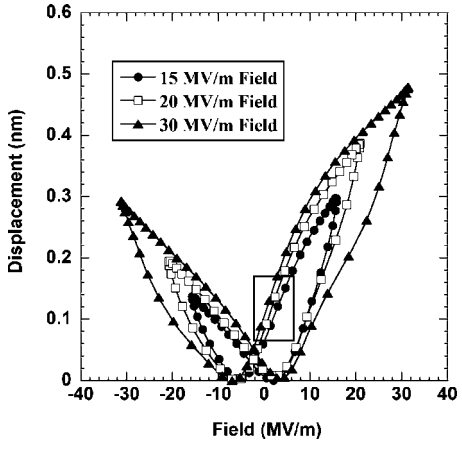

FIG. 3. Measured out-of-plane displacement for 350 nm film driven at increasing fields. The slope in the boxed region was used to calculate d_{33} values.

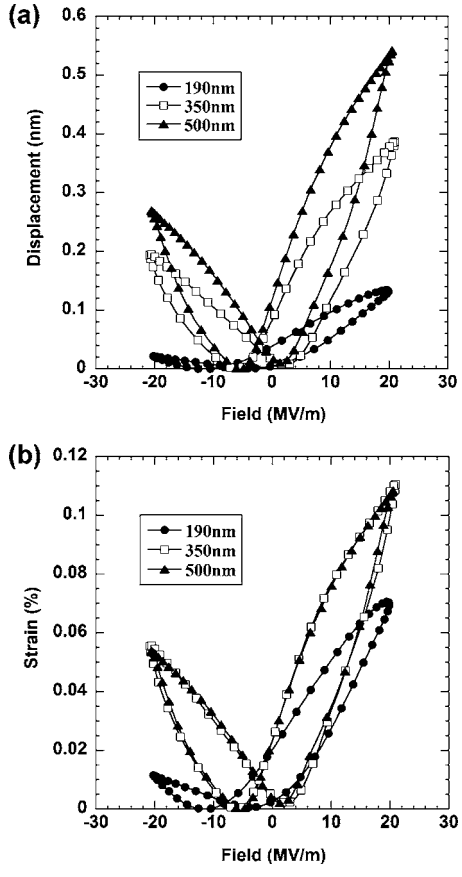

FIG. 4. Comparison of displacement-field loops (a) and strain-field loops (b) for the 190, 350, and 500 nm films driven at 20.0 MV/m.

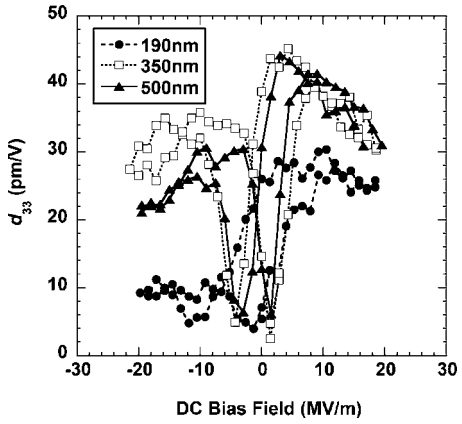

FIG. 5. Calculated d_{33} for a small ac voltage (1.0 MV/m) applied over a large dc bias voltage.

and negatively applied fields is also observed for both driving methods. As expected, higher displacements are observed for positive driving fields, in accordance with the film expanding away from the substrate. Less displacement amplitudes, and thus lower d_{33} values, are measured in the direction of negatively applied fields. The lower displacement is attributed to the constraint of the substrate while the film is being compressed.

IV. DISCUSSION

For each driving method, the residual stress significantly influences the piezoelectric behavior of the thin films. A reduction in piezoelectric response coincides with a decrease in thickness and an increase in the measured residual stress (Table I). While the coupled electromechanical response depends on many factors such as composition, grain size, processing stress, etc., it is expected to be independent of film thickness for specimens in which these other factors have been held constant. As shown by the strain-field response loops in Fig. 4(b), the 190 nm sample demonstrates a vastly diminished strain capability and a higher measured residual stress than the 350 and 500 nm specimens. If the thickness alone were the dominating factor influencing thin film piezoelectric properties, then an appreciable difference would also be expected between the strain-field responses of the 350 and 500 nm specimens. However, despite a thickness differential nearly the same as that between the 190 and 350 nm specimens (~160 nm), the strain-field performance for the 350 and 500 nm specimens is nearly identical. The suppressed strain-field response correlates with the increased residual stress level. This same trend is repeated for the dc bias measurements in Fig. 5. The observed dependence on residual stress state is also consistent with the previous findings of Lian and Sottos[8] who showed that an enhanced field-induced strain response (18%) could be achieved for PZT specimens in which some of the residual tensile stress (48 MPa) was relieved uniaxially. Some previous works[13,23] have shown a continued increase in piezoresponse with film thickness across this same regime of film thickness. In contrast, this work has shown a leveling off piezoresponse with increasing film thickness, which coincides with a nearly constant residual stress state. We postulate that differences in processing techniques during the film fabrication for these other works may result in a continued decrease in residual stress level as the film thickness increases, although the residual stress level is often not measured or reported.

For both the ac and dc bias driving cases, the measured d_{33} drops with increasing residual stress. However, Table I shows that a noticeable difference exists in the d_{33} value measured on the same specimen under different driving conditions. For the 350 and 500 nm specimens, there is a ~30% decrease in measured d_{33} for the dc bias case, while a similar 12% decrease is observed for the 190 nm sample. The origin of this difference is likely a combination of the active mechanisms that contribute to the piezoelectric response and the manner in which d_{33} is calculated for each of the respective driving cases. In the ac driving case, d_{33} is found from the linear portion of the displacement-field loop. For different ac field levels there is some variability in the slope of this region. While the variance is not large, nonlinear or inertial effects may influence the measured d_{33} value. The dc bias driving method likely provides a better measurement of the linear contributions to the piezoelectric response.

The components of the linear contribution include reversible displacements stemming from stretching of the unit cell dipoles and domain wall vibrations.[27] Part of the inhibiting effect of residual stress on the linear portion of the piezoelectric response is readily explained by the Poisson effect from classical mechanics. The basis of this principle is that for an infinitesimal element in a continuum, tensile loading in one principal direction will cause a contraction in the other two principal directions (for $\nu > 0$). In the case of these electroceramic thin films, out-of-plane displacements induced by a driving field in the three direction must be accompanied by a contraction in the 1-2 plane. Superimposing a high biaxial tensile stress in the 1-2 plane severely limits the amount of allowed contraction and thus reduces the potential out-of-plane strains possible through electrical loading. Therefore, a lower effective d_{33} will be measured for electroceramic thin films with high residual biaxial tensile stresses. Although the residual stress is assumed to be uniform across the film thickness, the potential for a stress gradient and interfacial effects may exist due to the layered deposition process. However, no evidence of grain size changes was found from SEM cross-sectional micrographs. In addition, a series-dilution model analysis[22] of the dielectric response determined that a constant impedance factor existed between the films, which indicates dense films with no variation in properties between layers.

Others have proposed that a further effect of high residual stresses is ferroelectric domain pinning.[28,29] Residual stress clamping hinders polarization switching and prevents domain wall motion, reducing the nonlinear contributions to the field-induced response. In bulk electroceramics, non-180° domain switching constitutes a large portion of the field-induced displacements[27] and is highly influenced by the specimen stress state.[30] The extent to which non-180° domain wall motions dictate piezoelectric response for thin films, however, is debatable. Previous research suggests that many nonlinear effects are minimized due to the constraint supplied by the substrate, which may also significantly im-

pede domain wall motion for films under 500 nm in thickness.[3,5] In addition, any domain wall switching present in the films under investigation would not be greatly favorable to the response in the three direction due to the (111) crystallographic orientation.

The potential for enhanced piezoresponse from switching of non-180° domains is appealing but is difficult to achieve for thin films. According to Tuttle *et al.*,[2,5] tensile stresses upon cooling from the Curie temperature create films that have high populations of *a*, or 90°, domains and that demonstrate a suppressed strain-field response. While the 53/47 composition thin films in this study are not highly tetragonal, any stress-driven preferential orientation of the polarization direction into the 1-2 plane would result in domains confined to this orientation by substrate constraints and high residual stresses. Consequently, there would be poor piezoelectric coupling and fewer domain switching sites available, minimizing any contribution to the piezoelectric response from nonlinear sources for thin films. Recently, Bühlmann *et al.*[31] reported dramatic increases in piezoresponse for patterned thin PZT films with feature sizes on the order of 100 nm. Similar results were observed by Nagarajan *et al.*[32] for PZT elements etched into discrete islands. In both of these studies, the etching processes provided relief of processing related residual stresses, as well as the material constraint provided by a continuous film. The stress release in these patterned films enabled 90° domain switching and therefore enhanced the field-induced strain response.

In the course of the dc-biased testing, the films are also driven out to biased field levels surpassing the noted saturation point, which results in a lowered displacement amplitude. This phenomenon is also observed in soft PZT bulk samples and attributed to domain pinning induced by the high dc field.[33] In this scenario, dipoles are in a highly stretched configuration as the dc bias field becomes larger. Continued increases in the applied dc field potentially lead to the domains becoming locked in this stressed arrangement and unable to respond to the small voltage fluctuations provided by the overlapping ac field. Thus, the extent and onset of this degradation in ferroelectric response are dependent on the magnitude of the applied ac ripple. A similar effect is observed for d_{33} estimates obtained from the instantaneous derivative of the displacement-voltage curves in the large applied ac field case. This d_{33} value reaches a peak in the constant slope region and then progressively decreases as more voltage is applied. The films appear to reach a saturation point, after which all domain switching has occurred and intrinsic dipole stretching has reached its limits.

V. CONCLUSIONS

Wafer curvature measurements were used to determine residual processing stresses for three sol-gel derived $Pb(Zr_{0.53}Ti_{0.47})O_3$ thin film samples. The effect of residual stresses on the piezoelectric response was investigated through the measurement of field-induced displacements for two different electrical driving methods. Under large ac loading, films with higher residual stress demonstrated a reduced strain-field response, and films with similar residual stress states demonstrated consistent piezoelectric behavior. The same trend was observed for the measured piezoelectric coefficient, d_{33}, which decreased for higher residual stresses under both driving cases. This behavior was attributed to the suppressing effect of residual stress on both linear and nonlinear components of the ferroelectric response, specifically hindering polarization switching and domain motions.

ACKNOWLEDGMENTS

The authors would like to acknowledge and thank the National Science Foundation for its funding of this research through Grant No. CMS 00-8206. Much of this work is based upon previous studies that have been supported by the U.S. Department of Energy, Division of Materials Sciences under Award No. DEFG02-91ER45439, through the Frederick Seitz Materials Research Laboratory at the University of Illinois at Urbana-Champaign.

[1] G. A. C. M. Spierings, G. J. Dormans, W. G. J. Moors, M. J. E. Ulenaers, and P. K. Larsen, J. Appl. Phys. **78**, 1926 (1995).
[2] B. A. Tuttle, J. A. Voigt, T. J. Garino, D. C. Goodnow, R. W. Schwartz, D. L. Lamppa, T. J. Headley, and M. O. Eatough, Applications of Ferroelectrics, ISAF 1992, Proceedings of the Eighth IEEE International Symposium, Greenville, SC (IEEE, New York, 1992), p. 344.
[3] F. Xu, S. Trolier-McKinstry, W. Ren, and B. Xu, J. Appl. Phys. **89**, 1336 (2001).
[4] P. Gerber, C. Kügeler, U. Böttger, and R. Waser, J. Appl. Phys. **95**, 4976 (2004).
[5] B. A. Tuttle, T. J. Garino, J. A. Voigt, T. J. Headley, D. Dimos, and M. O. Eatough, Science and Technology of Electroceramic Thin Films: Proceedings of the NATO Advanced Workshop, 1994, Villa Del Mare, Italy, edited by O. Auciello and R. Waser (Kluwer Academic Publishers, New York, 1995), p. 117.
[6] J. Lappalainen, J. Franti, and V. Lantto, J. Appl. Phys. **82**, 3469 (1997).
[7] T. J. Garino and M. Harrington, Mater. Res. Soc. Symp. Proc. **243**, 341 (1992).
[8] L. Lian and N. R. Sottos, J. Appl. Phys. **95**, 629 (2004).
[9] C. J. Brinker and G. W. Scherer, *Sol-gel Science: The Physics and Chemistry of Sol-gel Processing* (Academic Press, San Diego, 1990).
[10] K. R. Udayakumar, P. J. Schuele, J. Chen, S. B. Krupanidhi, and L. E. Cross, J. Appl. Phys. **77**, 3981 (1995).
[11] C. D. E. Lakeman and D. A. Payne, Ferroelectrics **152**, 145 (1994).
[12] F. Chu, F. Xu, J. Shepard, and S. Trolier-McKinstry, Mater. Res. Soc. Symp. Proc. **493**, 409 (1998).
[13] H. Maiwa and N. Ichinose, Jpn. J. Appl. Phys., Part 1 **42**, 4392 (2003).
[14] S. B. Ren, C. J. Lu, S. Liu, H. M. Shen, and Y. N. Wang, Phys. Rev. B **54**, R14337 (1996).
[15] D. Damjanovic, D. V. Taylor, and N. Setter, Mater. Res. Soc. Symp. Proc. **596**, 529 (2000).
[16] D. V. Taylor and D. Damjanovic, Appl. Phys. Lett. **76**, 1615 (2000).
[17] K. D. Budd, S. K. Dey, and D. A. Payne, Br. Ceram. Proc. **36**, 107 (1985).
[18] C. D. E. Lakeman and D. A. Payne, J. Am. Ceram. Soc. **75**, 3091 (1992).
[19] T. A. Berfield, R. Ong, N. R. Sottos, and D. A. Payne, Mater. Res. Soc. Symp. Proc. **784**, 29 (2003).
[20] G. A. C. M. Spierings, G. J. M. Dormans, W. G. J. Moors, M. J. E. Ulenaers, and P. K. Larsen, Applications of Ferroelectrics, ISAF 1994, Proceedings of the Ninth IEEE International Symposium, University Park, PA, 1994 (IEEE, New York, 1994), p. 29.
[21] L. Zhang, M. Ichiki, and R. Maeda, J. Eur. Ceram. Soc. **24**, 1673 (2004).
[22] R. J. Ong, N. R. Sottos, and D. A. Payne, J. Am. Ceram. Soc. **88**, 2839 (2005).
[23] L. Lian and N. R. Sottos, J. Appl. Phys. **87**, 3941 (2000).
[24] A. J. Moulson and J. M. Herbert, *Electroceramics: Materials, Properties, and Applications* (Chapman and Hall, London, 1990).
[25] R. J. Ong, T. A. Berfield, N. R. Sottos, and D. A. Payne, J. Eur. Ceram. Soc. **25**, 2247 (2005).
[26] R. J. Ong, Ph.D. thesis, University of Illinois at Urbana-Champaign, 2005.
[27] D. A. Hall, J. Mater. Sci. **36**, 4575 (2001).
[28] W. L. Warren, D. Dimos, B. A. Tuttle, G. E. Pike, M. V. Raymond, R. D.

Nasby, R. Ramesh, and J. T. Evans Jr., Mater. Res. Soc. Symp. Proc. **361**, 51 (1995).
[29]D. Liu, C. Wang, H. Zhang, J. Li, L. Zhao, and C. Bai, Surf. Interface Anal. **32**, 27 (2000).
[30]G. Yang, W. Ren, S. F. Liu, A. J. Masys, and B. K. Mukherjee, Proceedings of the 2000 IEEE Ultrasonics Symposium, San Juan, PR, Vol. 2, edited by S. C. Schneider, M. Levy, and B. R. McAvoy (IEEE, New York, 2000), p. 1005.
[31]S. Bühlmann, B. Dwir, J. Baborowski, and P. Muralt, Appl. Phys. Lett. **80**, 3195 (2002).
[32]V. Nagarajan, A. Roytburd, A. Stanishevsky, S. Prasertchoung, T. Zhao, L. Chen, J. Melngailis, O. Auciello, and R. Ramesh, Nat. Mater. **2**, 43 (2003).
[33]A. J. Masys, W. Ren, G. Yang, and B. K. Mukherjee, J. Appl. Phys. **94**, 1155 (2003).